

Communications in Physics, Vol. 26, No. 2 (2016), pp. 173-180

DOI:10.15625/0868-3166/26/2/8518

SYNTHESIS AND CHARACTERIZATION OF Ag/PEDOT:PSS FILMS USED FOR NH₃ SELECTIVE SENSING

LAM MINH LONG AND NGUYEN NANG DINH[†]

*University of Engineering and Technology, Vietnam National University Hanoi,
144 Xuan Thuy, Hanoi, Vietnam*

HOANG THI THU, HUYNH TRAN MY HOA AND TRAN QUANG TRUNG

*University of Natural Science, Vietnam National University, Ho Chi Minh City
227 Nguyen Van Cu Road, District 5, Ho Chi Minh City*

[†]E-mail: dinhnn@vnu.edu.vn

Received 15 July 2016

Accepted for publication 18 August 2016

Abstract. *Nano-Ag/PEDOT-PSS films were prepared by spin-coating technique. SEM surface morphology, Raman spectra and gas sensing of methanol, humidity and NH₃ were studied. The obtained results showed that the resistance of Ag/PEDOT:PSS sheets exposed to gases related to the generation of electrons from the gases adsorption that eliminated holes as the major carriers in PEDOT:PSS. For NH₃ gas the largest change of the resistance of Ag/PEDOT:PSS was observed. The less sensitivity of humidity and ethanol sensing was explained due to less dedoping reaction between H₂O and ethanol vapor with Ag/PEDOT:PSS, respectively. This suggests a potential application of the nano-Ag/PEDOT-PSS sensors for the selective monitoring NH₃ gas in environment.*

Keywords: *PEDOT:PSS film; Raman spectra; gas sensing; NH₃ gas sensors.*

Classification numbers: *78.30.C-; 73.50.-h; 74.25.nd; 07.07.Df.*

I. INTRODUCTION

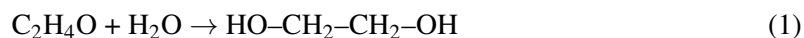
Nanocomposites are known as materials mixing two or more different materials, where at least one of these having a nano-dimensional phase, for example, conducting polymers embedded with metallic, semiconducting, and dielectric nanoparticles. In comparison with devices made from standard materials, the nanocomposites-based devices usually possess enhanced efficiency and service life [1–4]. If metallic nanoparticles are embedded in the conducting polymer, new active sites are generally created for *in-situ* trapping of electrons [5]. Polypyrrole (PPy)/Ag has been shown to be an excellent ammonia gas sensor which can sense the gas down to 10 ppm [6].

Similarly, noble metal nanoparticles with PPy have been reported to be an excellent candidate as sensor materials for stable enzyme biosensors based on chemically synthesized Au-polypyrrole nano-composites [7]. Monitoring of ammonia (NH₃) and hydrogen sulphide (H₂S) gas is of great industrial importance as well as of social impact. Conducting PPy is a p-type semiconductor and its doping and un-doping with gaseous molecules e.g., ammonia leads to reversible redox reactions. It is reported that the interaction of NH₃ with PPy results in formation of the neutral polymer backbones due to decrease in the charge-carrier concentration which consequently results in decrease and/or increase in conductivity of PPy reversibly [8]. The effects of film thickness, annealing temperature and CNTs content on gas-sensing response of PPy-CNTs nanocomposite for detection of NH₃ gas at room temperature were investigated in Ref. [9].

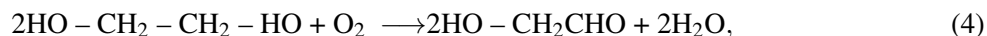
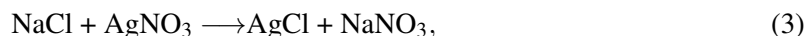
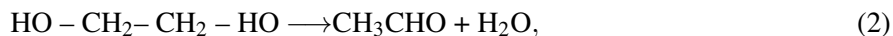
Poly(3,4-ethylenedioxythiophene):poly(styrenesulfonate) (PEDOT:PSS) has a high transmission in the visible region, a high conductivity [10, 11] and a particularly good thermal stability. Thus PEDOT:PSS has received increasing interest in recent years. In PEDOT:PSS the conjugated polymer PEDOT is positively doped; the charge is balanced by the sulfonate anionic group in the PSS. The electrical conductivity of this conducting polymer blend reaches up to 80 S/cm [12], making it useful as plastic electrodes in optoelectronic devices. With a change in the conductivity when adsorbed by various gases, PEDOT:PSS can be used for the functional materials in the gases sensors [13]. In the hope to enhance the selectivity of the NH₃-gas sensor made from PEDOT:PSS, Ag-nanoparticles were embedded into PEDOT:PSS films in the present work.

II. EXPERIMENTAL

We used ethylene glycol (C₂H₆O₂) abbreviated to EG as a catalyst agent for synthesizing Ag nanoparticles. Basing on the fact that ethylene glycol (C₂H₆O₂) is produced from ethylene (ethene), via the intermediate ethylene oxide, ethylene oxide reacts with water to produce ethylene glycol according to the chemical equation:



20 ml of EG was filled in a glass, and magnetically stirred at 45°C for 15 min, then 17 mg of NaCl was added to the EG solvent to get NaCl+EG mixture. Heating the last to 100°C, 20 mg of AgNO₃ was put into the mixture. The reaction between NaCl and AgNO₃ gave a product of an AgCl opaque solution. While EG decomposed to its andehist and played a role of reducing agent for forming AgCl served as nuclear in the Ag-nanoparticles growth. This process can be written by following reactions:



The last solution (namely the product of Eq. (5)) is called EGH and kept at maintained value of pH = 6. Next, PEDOT:PSS solution (1-3 wt.%, Clevios Ltd.) was prepared by mixing 1 ml of PEDOT:PSS and 10 ml of distilled water, then stirred for 1.5 h by using ultrasonic machine. The EGH was dropped into the PEDOT:PSS solutions according a volume ration of 1:1 and ultrasonically stirred for 1 h to get completely a homogenous EGH +PEDOT:PSS solution. Using

spin-coating, this solution was deposited onto glass substrates which were coated by two silver planar electrode arrays with a square of $5 \times 5 \text{ mm}^2$ in size, as shown in Fig. 1. Two electrodes are separated each from other in a distance (l) of 5 mm. In the spin-coating technique used for preparing composite films, following parameters were chosen: a delay time of 120 s, a rest time of 30s, a spin speed of 1200 – 1500 rpm, an acceleration of 600 rpm, and finally a drying time of 5 min. To dry the films, the last were put in a flow of dried gaseous nitrogen for 8 hours. For the solidification with completely avoiding the solvents, the film samples were annealed at 120°C for 8h in a “SPT-200” vacuum drier. The obtained Ag/PEDOT:PSS composite films were abbreviated to PEAC.

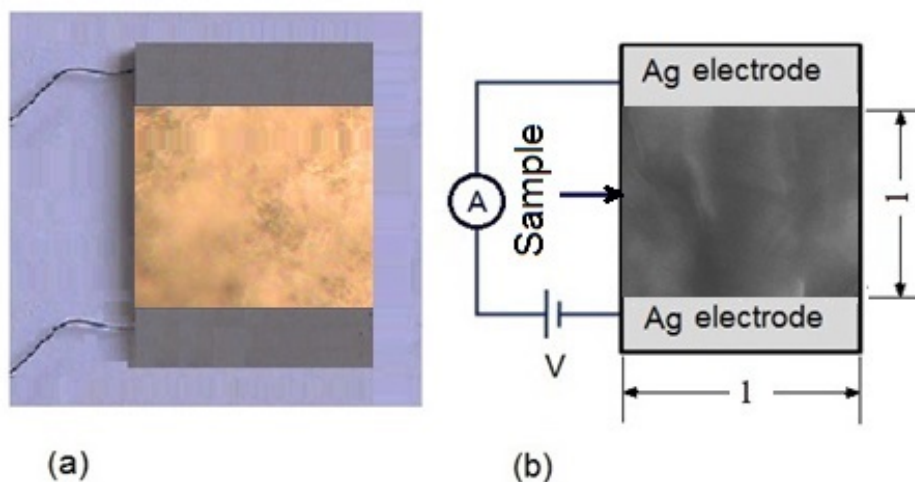


Fig. 1. Image of a gas sensor made from the PEAC film (a) and the schematic drawing of the device with the two planar electrodes (b). Resistance change is detected by the change in the current with a constant Dc-bias applied to the two electrodes.

The thickness of the films was measured on a “Veeco Dektak 6M” stylus profilometer, for all samples the film thickness was of about $3 \mu\text{m}$. The surface morphology of the films was characterized by using Emission Scanning Electron Microscopy (FE-SEM). FTIR data were obtained from measurements on a BRUKER TENSOR-27 spectrometer.

For monitoring gases, the prepared sensing samples were put in a testing chamber of 10dm^3 in volume. The gases value can be fixed in a rage from 100 to 1000 ppm by use of an “EPA-2TH” profilometer (USA). The adsorption process was controlled by insertion of measuring gases and the desorption process was done by extraction of the gases followed by insertion of dry gaseous Ar. The measurement system that was described in Ref. [14] consists of an Ar gas tank, gas/vapor hoses and solenoids system, two flow-meters, a bubbler with vapor solution and an airtight test chamber connected with collect-store data DAQ component. The Ar gas played a role as carrier gas, dilution gas and purge gas.

III. RESULTS AND DISCUSSION

The films created during electrodeposition were light blue in color, and would turn darker as the electrodeposition continued in time. Figure 2 is a FE-SEM micrograph of the PEAC sample, the presence of Ag nanoparticles made the sample surface rough, instead of smooth one as usually observed for the pure PEDOT:PSS conjugate polymer film [15]. In this work, it was shown that in the pure conjugate polymer nano-scale cracked spots were often created during the post-annealing, whereas, for the composite film with embedded TiO₂ nanoparticles, no similar spots could be observed. Similarly to this, for the as-prepared PEDOT:PSS film, some spots were formed. After annealing at high temperatures these spots were considerably expanded, whereas in the PEAC composite film no cracked spots were observed.

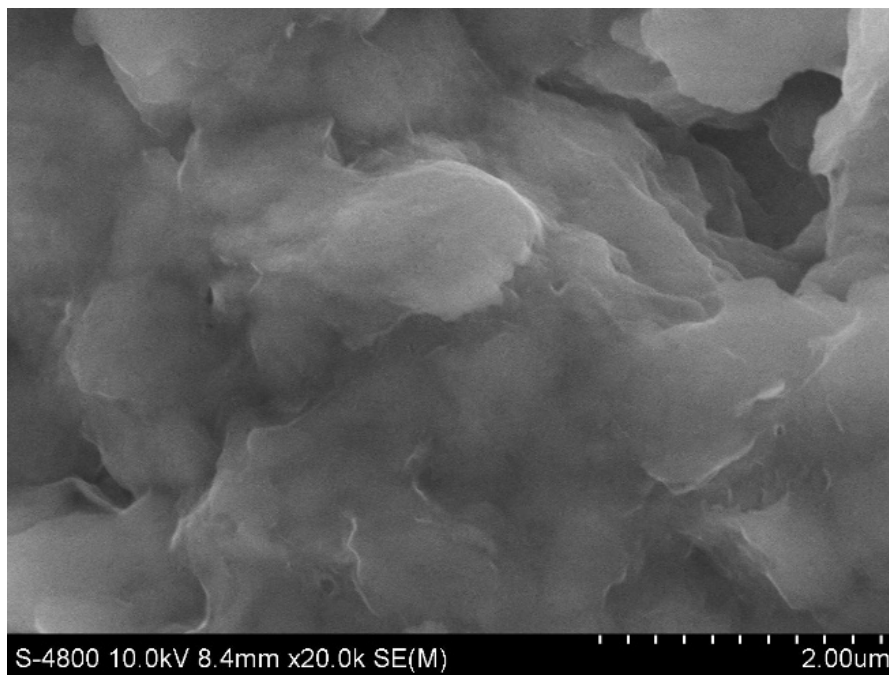


Fig. 2. FE-SEM micrograph of the PEAC sample.

Characterization of the PEDOT:PSS films was done through Fourier Transform Infrared Spectroscopy (FTIR). Figure 3 shows the FTIR spectra obtained for a PEAC film sample. Signals from 1527 to 1368 cm⁻¹ are associated with the C=C bonds, peaks at 985, 844, and 688 cm⁻¹ can be attributed to the C-S interaction in the thiophene ring, and peaks 1228 through 1051 cm⁻¹ correspond to the ethylenedioxy group. Besides, silver nanoparticles exhibited prominent peaks signals from 1652 to 1051 cm⁻¹. More detailed data of the FTIR are listed in Table 1. From Table 1 it is seen that among 16 peaks observed there are 12 characteristic peaks belong to PEDOT:PSS [16] and only 4 peaks belong to nanosilver as obtained for silver nanoparticles synthesized from *myxococcus virescens* and their lethality on pathogenic bacterial cells [17].

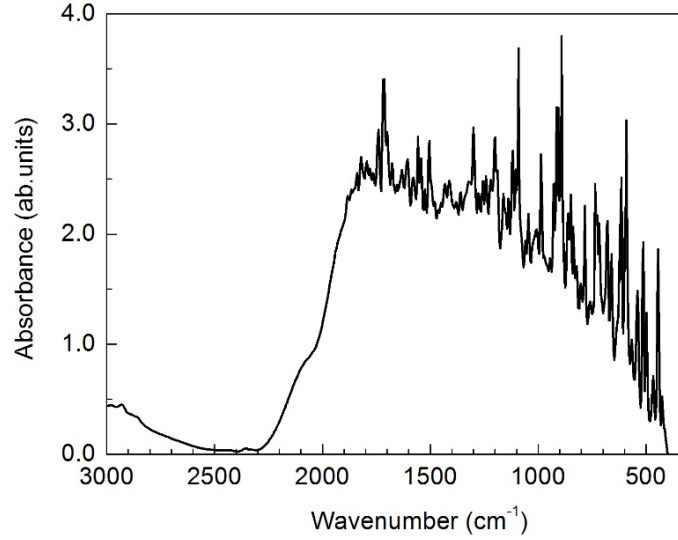


Fig. 3. A FTIR spectrum of the Ag/PEDOT:PSS (PEAC) sample.

Using four point probe technique, the resistivity (ρ) of the PEAC film was determined. The measurement of bulk resistivity is similar to that of sheet resistivity except that a resistivity in cm^{-3} is reported using the wafer thickness (t):

$$\rho = \frac{\pi}{\ln 2} t \left(\frac{V}{I} \right) = 4.523t \left(\frac{V}{I} \right) \quad (6)$$

where t is the layer/wafer thickness in cm. The simple formula above works for when the wafer thickness less than half the probe spacing [18]. From the results of measurements, $V = 100$ mV and $I = 5.03$ mA, the resistivity determined by formula (6) was found to be of $0.027 \Omega \cdot \text{cm}$, thus the conductivity ($\sigma \sim 1/\rho$) is of ca. 37 S/cm . This value of the conductivity of the PEAC film can be compatible to the one of a composite film made from graphene quantum dots, PEDOT:PSS and carbon nanotubes as reported in [19] and much less than the pure PEDOT:PSS film [12]. Embedding Ag nanoparticles into PEDOT-PSS have made the conductivity of PEDOT-PSS decreased, leading to the expectation that the sensitivity of the PEAC composite films would be enhanced.

To clearer understand the sensing performance of the PEAC films used for the sensors, a sensing response (η) of the devices was introduced. It is determined by following equation:

$$\eta = \frac{R - R_0}{R_0} (\%) \quad (7)$$

where R_0 is the initial resistance of the PEAC sensor, namely $23.10 \text{ k}\Omega$.

To characterize gas sensitivity of the samples, the devices were placed in a test chamber and device electrodes were connected to electrical feedthroughs. The measurements included two processes: adsorption and desorption. In the adsorption process, the gas (or vapor) flow consisting of Ar carrier and measuring vapor from a bubbler was introduced into the test chamber for an interval of time, following which the change in resistance of the sensors was recorded. In the

Table 1. FTIR data of PEAC compared to Ag nanoparticles and PEDOT:PSS.

No.	Ag/PEDOT:PSS [This work]	PEDOT:PSS [16]	Nano Ag [17]
1	1648.71 [†]		1652
2	1535.27		1539
3	1523.43 ^{*,†}	1527	
4	1421.70 [*]	1425	
5	1363.83 [?]	1368	1386
6	1223.54 [*]	1228	
7	1103.67 [*]	1109	
8	1091.63 [†]		1051
9	1047.38 [*]	1051	
10	983.52 [*]	985	
11	921.23 [*]	923	
12	848.65 [*]	844	
13	796.93 [*]	798	
14	683.91 [*]	688	
15	661.63 [*]	667	
16	590.05 [†]		582

“*” corresponds to PEDOT:PSS and “†”- to Ag nanoparticles.

desorption process, a dried Ar gas flow was inserted in the chamber in order to recover the initial resistance of the sensors. Through the recovering time dependence of the resistance one can obtain information on the desorption ability of the sensor in the desorption process.

The PEAC film sensors were exposed to methanol, humidity vapor and NH₃ gas with 300 ppm, 200 ppm and 100 ppm concentrations, respectively. Typical sensor response data are plotted in Fig. 4.

The responding time of all the samples is about 30s and the resistances of the composite films fast recovered to baseline when exposed to air. In the same of the period of time (namely 50 s), the sensing response to methanol, humidity and NH₃ attained a value of 0.5, 0.7 and 5.5, respectively. In the subsequent cycles, the humidity desorption/adsorption process led respectively to increase and decrease of the resistance of sensors, with results similar to those reported in [13]. However, through each cycle, the resistance of the sensors did not recover/restore to its initial value, but increased in 0.10 to 0.20 kΩ, to a final value of 25.40 kΩ after 500s from 23.10 kΩ (for NH₃ gas). The largest increase in the initial resistance of Ag/PEDOT:PSS exposed to NH₃ mainly related to the decrease of the major charge carriers in PEDOT:PSS [20]. This is due to the elimination of holes (as the major carriers in PEDOT:PSS) by electrons that were generated from the NH₃ adsorption. The more desorption/adsorption cycles, the more holes were eliminated in the deeper distances in the composite films. For Ag/PPy based sensors, the vapors of NH₃ gas will interact with the Ag/PPy nano-composite film causing a dedoping reaction thus increasing the fraction of neutral polymer chains through electron-donating ability of ammonia, to the oxidized

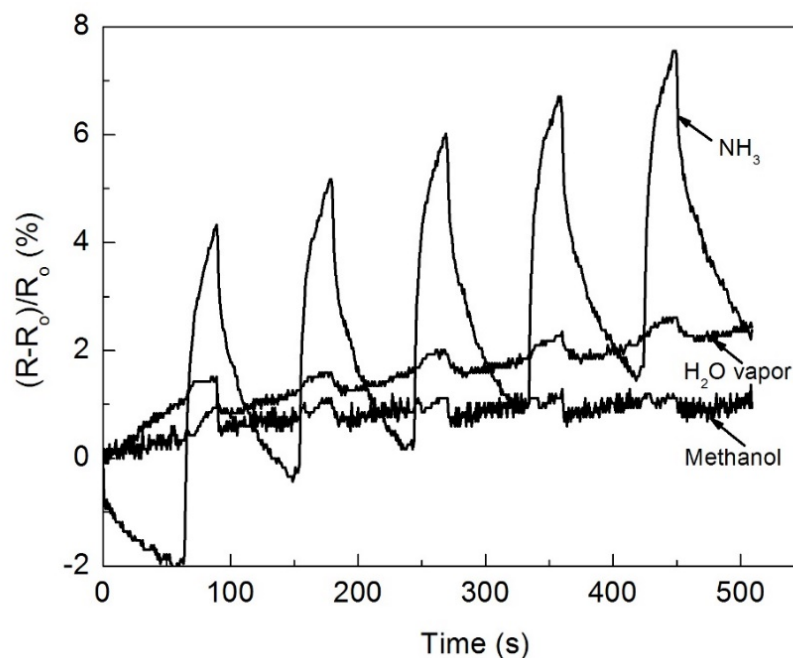


Fig. 4. Comparison of the sensitivities of the sensors responding to methanol, humidity and NH_3 .

(positively charged) polymer chains. This therefore will decrease the electrical conductivity due to the decrement in charge carrier density [21]. As conducting polymer PEDOT:PSS is a p-type organic semiconductor, with Ag/PEDOT:PSS composite thick films used for monitoring NH_3 , the similar behavior in NH_3 sensing was exhibited. The fact that the sensitivity of humidity and ethanol sensing was much smaller than that of the NH_3 sensing can be attributed to less dedoping reaction between H_2O and ethanol vapor with Ag/PEDOT:PSS.

IV. CONCLUSION

Using spin-coating technique the films of PEDOT-PSS embedded with Ag-nanoparticles were prepared for NH_3 -gas sensors. The surface morphology, Raman spectra and gas sensing of methanol, humidity and NH_3 were characterized. The obtained results showed that the increase in the initial resistance of Ag/PEDOT:PSS exposed to gases mainly related to the decrease of the major charge carriers in PEDOT:PSS. With the NH_3 gas the largest change of the resistance of Ag/PEDOT:PSS was observed. The less sensitivity of humidity and ethanol sensing was explained due to less dedoping reaction between H_2O and ethanol vapor with Ag/PEDOT:PSS, respectively.

ACKNOWLEDGEMENTS

This research was funded by the Vietnam National Foundation for Science and Technology (NAFOSTED) under grant number 103.02-2013.39. The author (L. M. Long) expresses sincere

thanks to University of Science, VNU in Ho Chi Minh city for the support in experimental measurements.

REFERENCES

- [1] T. P. Selvin, J. Kuruvilla and T. Sabu, *Mater. Lett.* **58** (2004) 281.
- [2] J. Móczó and B. Pukánszky, *J. Ind. Eng. Chem.* **14** (2008) 535.
- [3] S. A. Choulis, M. K. Mathai and V.-E. Choong, *App. Phys. Lett.* **88** (2006) 213503.
- [4] T. T. Thao, T. Q. Trung, V.-V. Truong and N. N. Dinh, *J. Nanomater.* **2015** (2015) 151.
- [5] R. Brina, G. E. Collins, P. A. Lee and N. R. Armstrong, *Anal. Chem.* **62** (1990) 2357.
- [6] X. Yang, L. Li and F. Yan, *Sens. Actuators B: Chem.* **145** (2010) 495.
- [7] J. Njagi and S. Andreescu, *Biosensors and Bioelectronics* **23** (2007) 168.
- [8] H. Bai, L. Zhao, C. Lu, C. Li and G. Shi, *Polymer* **50** (2009) 3292.
- [9] N. Van Hieu, N. Q. Dung, P. D. Tam, T. Trung and N. D. Chien, *Sens. Actuators B: Chem.* **140** (2009) 500.
- [10] J. Ouyang, Q. Xu, C.-W. Chu, Y. Yang, G. Li and J. Shinar, *Polymer* **45** (2004) 8443.
- [11] P. Tehrani, A. Kancierzewska, X. Crispin, N. D. Robinson, M. Fahlman and M. Berggren, *Solid State Ionics* **177** (2007) 3521.
- [12] J. Ouyang, C.-W. Chu, F.-C. Chen, Q. Xu and Y. Yang, *Adv. Funct. Mater.* **15** (2005) 203.
- [13] J. N. Gavvani, H. S. Dehsari, A. Hasani, M. Mahyari, E. K. Shalamzari, A. Salehi and F. A. Taromi, *RSC Advances* **5** (2015) 57559.
- [14] T. Sreepasad, A. A. Rodriguez, J. Colston, A. Graham, E. Shishkin, V. Pallem and V. Berry, *Nano Lett.* **13** (2013) 1757.
- [15] N. N. Dinh, L. H. Chi, T. T. C. Thuy, T. Q. Trung, V.-V. Truong et al., *J. Appl. Phys.* **105** (2009) 093518.
- [16] S. V. Selvaganesh, J. Mathiyarasu, K. Phani and V. Yegnaraman, *Nanoscale Research Letters* **2** (2007) 546.
- [17] W. Wrótniak-Drzewiecka, S. Gaikwad, D. Laskowski, H. Dahm, J. Niedojadło, A. Gade and M. Rai, *Austin J. Biotechnol. Bioeng.* **1** (2014) 01.
- [18] D. K. Schroder, *Semiconductor material and device characterization*, 3rd ed., John Wiley & Sons, 2006.
- [19] L. M. Long, N. N. Dinh and T. Q. Trung, *J. Nanomater.* **2016** (2016) .
- [20] J. Jang, M. Chang and H. Yoon, *Advanced Materials* **17** (2005) 1616.
- [21] B. Lundberg and B. Sundqvist, *J. Appl. Phys.* **60** (1986) 1074.